CFD SIMULATION FOR REDUCTION THROMBOSIS IN BILEAFLET MECHANICAL HEART VALVE USING VORTEX GENERATORS

NURSYAIRA MOHD SALLEH[1],
MOHAMAD SHUKRI ZAKARIA[1,2,*], MOHD JUZAILA ABD LATIF[1,3]

[1]Fakulti Kejuruteraan Mekanikal, Universiti Teknikal Malaysia Melaka,
Hang Tuah Jaya, 76100 Durian Tunggal, Melaka, Malaysia
[2]Centre for Advanced Research on Energy, Universiti Teknikal Malaysia Melaka,
Hang Tuah Jaya, 76100 Durian Tunggal, Melaka, Malaysia
[3]Advanced Manufacturing Centre, Universiti Teknikal Malaysia Melaka,
Hang Tuah Jaya, 76100 Durian Tunggal, Melaka, Malaysia
*Corresponding Author: mohamad.shukri@utem.edu.my

Abstract

Present study was done to investigate the performance of steady state flow through bileaflet mechanical heart valve (BMHV) with fixed fully open leaflet that equipped with vortex generator (VG) by using computational fluid dynamic (CFD) method. The VGs as a passive flow device that can improve the pressure gradient and reducing turbulent are investigated. For better understanding, the implications that VGs has on the blood flow through these valve, analysis of flow characteristic such as velocity and pressure drop was performed. The novelty of this study is to determine the performance of VGs configurations affect the computed velocity and pressure gradient associated with the development of the blood clotting. The laminar flow cases that computed mean velocity profile are done validate close to the experimental result. Results suggested that triangular VGs caused increase velocities and reduce pressure drop. The straight triangular VGs showed lower pressure drop and 5.3% improvement in pressure drop. percentage.

Keywords: Bi-leaflet mechanical valves, Computational fluid dynamics, Pressure drop, Thrombosis, Vortex generator.

1. Introduction

Complications arise when using artificial prosthetic heart valves, such as bioprosthetic heart valve or mechanical heart valve (MHV), as replacement in heart valve diseases. The most common replacement used in the world is bileaflet mechanical heart valve because their design can minimize flow disturbance (BMHV) [1]. However, replacing BMHV causes major complications, such as thrombosis (blood clotting) and bleeding, even though the design of BMHV already been improved [2]. Warfarin is a medicine that can treat blood clotting, but this medicine should be taken at the right dosage to prevent the development of haemorrhage [3]. The medicine may change the lifestyle of the patient which they will encounter a problem when injured or requires surgery especially during the surgery it will cause excessive bleeding if not control the dosage of medicine.

The problem with blood clotting also can be treated by using vortex generator (VGs) as a passive flow device which can control the non-physiological flow in the vicinity of heart valve. Therefore, the analysis of non-physiological flow through BMHV are important to determine blood cell damage because it will initiate thrombus formation [4]. Ge et al. [5] investigated the numerical simulation of instantaneous limiting streamlines, contours of wall shear stress magnitude along the sinus wall and velocity field which are not available by experimental methods. Then they used detached eddy simulation (DES) approaches to reveals the unknown features of the flow that it is potential as a powerful modeling tool of cardiovascular flows at physiological conditions.

Thrombosis complication can be reduced by converting the valves into thrombus-resistant materials or adding a vortex generator (VG) on the leaflet to lessen the use of warfarin. Previous study analysed the blood material interactions rendering a BMHV with superhydrophobic coating. Bark et al. [6] explored ways of superhydrophobic coating experiment with a receding contact angle of 160º strikingly could eliminates platelet and leukocyte adhesion to the surface. Superhydrophobic BMHV has the potential to relax the requirement for antiplatelet and anticoagulant drug regimens typically required for patients receiving MHVs by minimizing blood-material interaction. Another study investigated passive flow control device that applied to BMHV could optimizes leakage flow hemodynamics at length scales that relevant to blood damage and platelet activation [7, 8].

Dasi et al. [7] analysed rectangular and hemispherical VG using particle high velocimetry (PIV) technique under pulsatile and steady flow condition. This study presents the significant diminution of turbulence stresses, specifically with the rectangular VG configuration. Then, Hatoum et al. [8] reported that rectangular VG configuration under pulsatile flow condition using PIV technique could improve pressure gradient and reducing turbulent. This study using rectangular VGs through different arrangement to generate a more delayed flow separation and more homogenized, streamline transition of flow. The application of VGs as a passive flow device in heart valve replacement contribute for controlling the development of blood clots by improving the hemodynamics of the valve.

The objective of this study is to investigate the performance of blood flow through BMHV at different level of triangular VGs configuration by reporting the relevant flow structure using contour and vector information, calculating the changes of pressure drop and comparing the result of pressure drop with triangular VGs configuration. The numerical simulation was performed on SJM valve model as a

prosthetic replacement for the aortic heart valve as shown in Fig. 1. In current study, Computational Fluid Dynamics (CFD) is used to model the valves and blood flows as the software allows relatively easy and economical conduction of parametric studies. This study also could provide data that can enhance our understanding of the VGs application which can lead to improve the design of MHV.
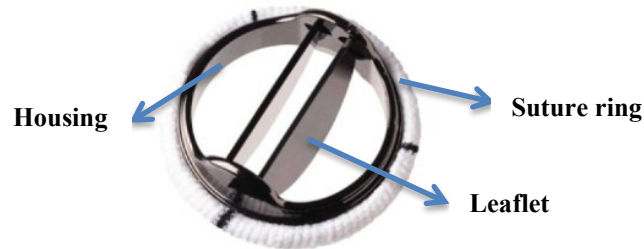

Fig. 1. The St. Jude Medical (SJM) valve model [6].

2. Numerical Method

The numerical method that used to develop the SJM valve laminar flow pattern was performed by solving the Navier-Stokes equation. The equation provides information on instantaneous velocity and pressure distribution. The application to solving the equation in medical field was previously used extensively in solving in other engineering area such as wind turbine [9], pipe flow [10], hydraulic [11], etc. The equations discuss the Navier-Stokes equations in differential form that obtained by using an infinitesimal control volume moving along a streamline with velocity vector $\vec{V} = (u, v, w)$ equal to the flow velocity at each point. For the three-dimensional incompressible flow, the continuity in Eq. (1) and three momentum equation is shown in Eqs. (2) to (4) [12].

$$\frac{\partial u}{\partial x} + \frac{\partial v}{\partial y} + \frac{\partial w}{\partial z} = 0 \tag{1}$$

$$\rho \frac{Du}{Dt} = -\frac{\partial p}{\partial x} + \left(\frac{\partial \sigma_{xx}}{\partial x} + \frac{\partial \sigma_{xy}}{\partial y} + \frac{\partial \sigma_{xz}}{\partial z} \right) + \rho f_x \tag{2}$$

$$\rho \frac{Dv}{Dt} = -\frac{\partial p}{\partial y} + \left(\frac{\partial \sigma_{yx}}{\partial x} + \frac{\partial \sigma_{yy}}{\partial y} + \frac{\partial \sigma_{yz}}{\partial z} \right) + \rho f_y \tag{3}$$

$$\rho \frac{Dw}{Dt} = -\frac{\partial p}{\partial z} + \left(\frac{\partial \sigma_{zx}}{\partial x} + \frac{\partial \sigma_{zy}}{\partial y} + \frac{\partial \sigma_{zz}}{\partial z} \right) + \rho f_z \tag{4}$$

where Eq. (1) is the continuity equation, and Eqs. (2), (3) and (4) are momentum equations in y. In equation above, ρ is the density of fluid, D/D_t is the material derivative and p is a pressure that present in a fluid at rest and acts normal to a surface and viscous stress which act normal to a surface or tangentially (shear stress). The pressure drop value can be calculated by identifying the pressure value in the simulation result. The pressure drop equation is non-dimensional ΔP coefficient equation, as shown in Eq. (5).

$$\Delta P = \left[(P_1 - P_2) / (\tfrac{1}{2} \rho V^2) \right] \tag{5}$$

where V is the average velocity, P_1 is the pressure at the leading edge of the leaflet, P_2 is the pressure at trailing edge of the leaflets and ρ is the blood density.

Numerical geometry

The geometry of the SJM valve as a prosthetic replacement for the aortic heart valve is shown in Fig. 2, with an inlet and outlet diameter of 25.4 mm representing the idealized aortic sinus root [2, 5]. The geometric model using aortic root contained a single axisymmetric sinus. The SJM valve has an orifice internal diameter of 20.4 mm and is geometrically identical to the prostheses implanted to the patients. The leaflet of the valve is fully open at an angle of 85° along the y-z plane.
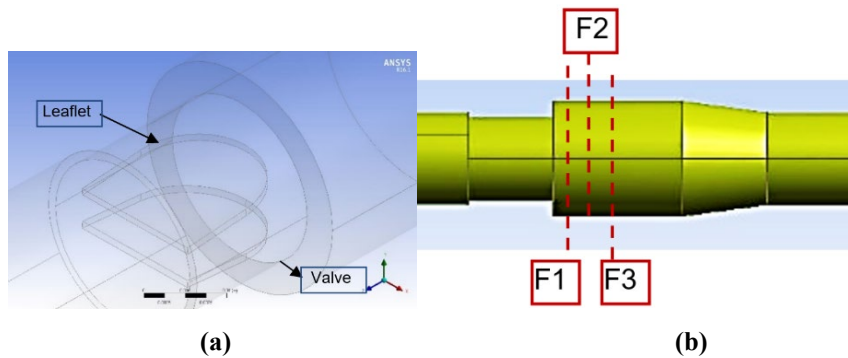

Fig. 2. Numerical geometry: (a) plan view of streamwise vertical axis at three different locations (F1-F3) and (b) geometry of SJM valve.

The VG geometry with triangular shape mounted on the downstream side of SJM valve with different arrangements was chosen in this study. Figure 3 shows the two different VG arrangements where the model of the valve is designed using Solidwork 2018. The base VG dimensions were chosen to be 1 mm of thickness, height 1 mm and length 4 mm based on Hatoum et al. [8].
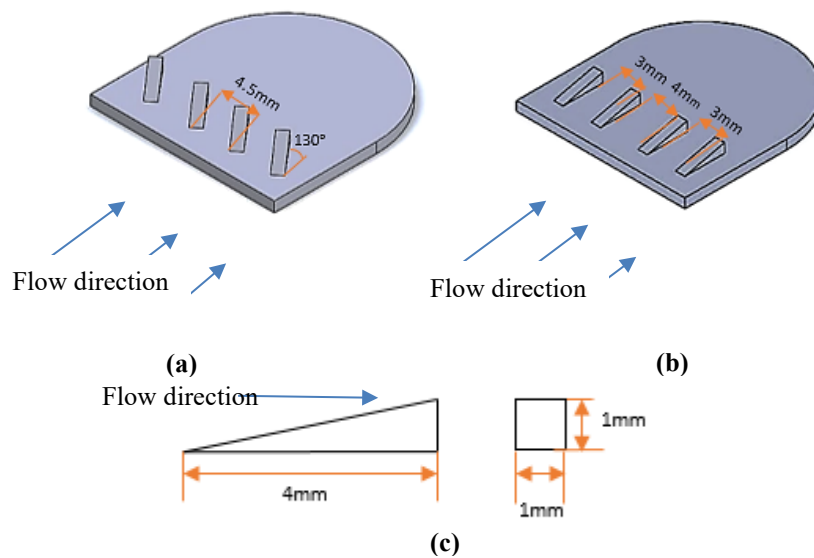

Fig. 3. VG leaflet arrangement: (a) equally triangular VG (b) straight triangular VG (c) triangular VG dimension.

For the meshing process, the maximum value of the skewness is ideally less than 0.85 [13]. For this study, the number of nodes 482K and elements 2M provide maximum value of skewness is 0.83 that show it is good quality of meshing. This study used a mesh configuration with tetrahedron shape. This configuration has a maximum mesh size of 0.0004 m. This method was used to assure that the mesh configuration can produce good simulation result. The mesh configuration of the geometry is shown in Fig. 4, by using ANSYS meshing application.
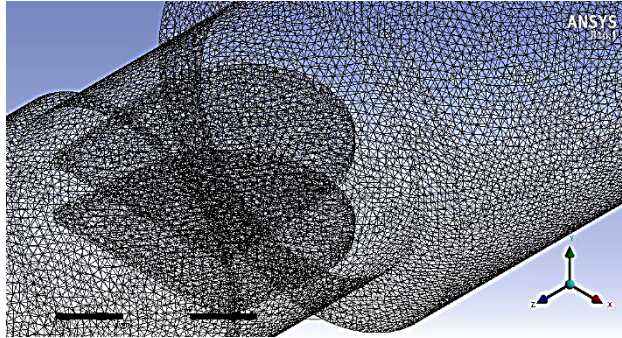

Fig. 4. Mesh configuration of SJM valve.

Figure 5 shows the grid-independent test study of the SJM valve for steady state solution at Re = 750. The velocity in stream-wise direction at the downstream of the leaflet at central plane (x = 0 mm) was computed (see Fig. 6, for plotted location). The velocity profile becomes grid-independent with increasing total number of elements [14]. Although choosing a large grid number 1.3 M is sufficient, the model with 1.08 M was chosen for mesh generation due to slight difference in the velocity profile.
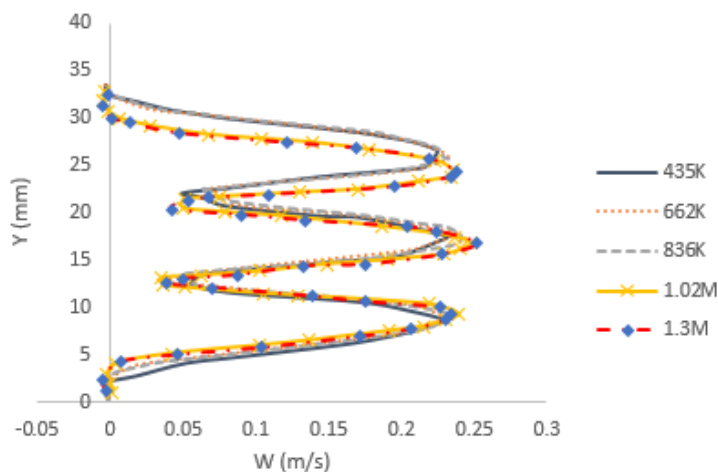

Fig. 5. Grid independent test.

The fluid used in the simulation had a density of 1060 kg/m^3 and dynamic viscosity of 5.5×10^{-3} kg/ms [5]. The boundary conditions were set with inlet, outlet and wall domain at the geometry as following.

At the inlet of the domain, the velocity inlet, V (m/s) was set with user-defined function (UDF) at the center of the z-plane. The inlet boundary conditions were assumed according to the parabolic profile in the boundary layer by setting the velocity profile to compute the non-uniform velocity distribution at the inlet.

Reynolds number is defined as Re $= V_{avg}D/v$, where D is the inlet diameter, v is the kinematic viscosity and V_{avg} is the average velocity [6]. The reference inlet was set at a fully developed velocity with $V_{avg} = 2/3 V_{max}$ and 25.4 mm of inlet diameter.

The radius from the central axis of parabola was calculated using Eq. (6). The parabolic inlet boundary equation was derived as a velocity profile equation in Eq. (7).

$$r = \sqrt{(x[0] - x_0)^2 + (x[1] - y_0)^2 + (x[2] - z_0)^2} \qquad (6)$$

$$V_{profile} = V_{peak} \left(1 - \left(\frac{r}{R}\right)^2\right) \qquad (7)$$

where r is the radius from central axis of parabola, and R is the maximum radius of the valve.

A pressure outlet in the domain was applied with a pressure gauge of zero pascal because of the same effect generated by the difference in fluid distribution function in the flow [15]. The domain wall was set to no-slip shear condition because the wall motion is stationary.

The discretization scheme was a phase-coupled Semi-Implicit Method for Pressure Linked Equations (SIMPLE) for pressure-velocity coupling in the Navier stokes equation, least square cell based for the gradient, second order for pressure and second order upwind for momentum. The solution control was 0.3 for pressure and 0.7 for momentum under relaxation factors. The convergence criteria were set to 1x10-6 to achieve the convergence. The calculation was computed until reaching the steady state.

There are several assumptions that are made by simplifying the fundamental equations in order to approximate blood flow characteristic of the domain. The assumption for blood flow through BMHVs are incompressible fluid with constant density that assumed to behave as Newtonian fluid [16]. This is because the main constituent of blood is the plasma where it is has properties of Newtonian fluid that the shear rate is linear, then this assumption is considered valid [17].

3. Validation and Verification

The numerical method was validated to determine the accuracy and ability of the method to produce accurate flow physics. The results were compared with the available experimental data [5]. The capabilities of the model were compared in Fig. 6. The graph was found in computed steady state condition with stream-wise velocity profiles (physical velocity) and three different locations (F1-F3) shown in Fig. 2, at different planes parallel to the leaflet (central planes, 0.3R mm and 0.6 R) for the Re = 750 case. The 25.4 mm value of R referred to the radius of the inlet diameter for SJM valve. The root mean square (RMS) is calculated to quantify the difference between computational and experimental results. The RMS of the velocity profile difference was 2.5% of the maximum velocity.
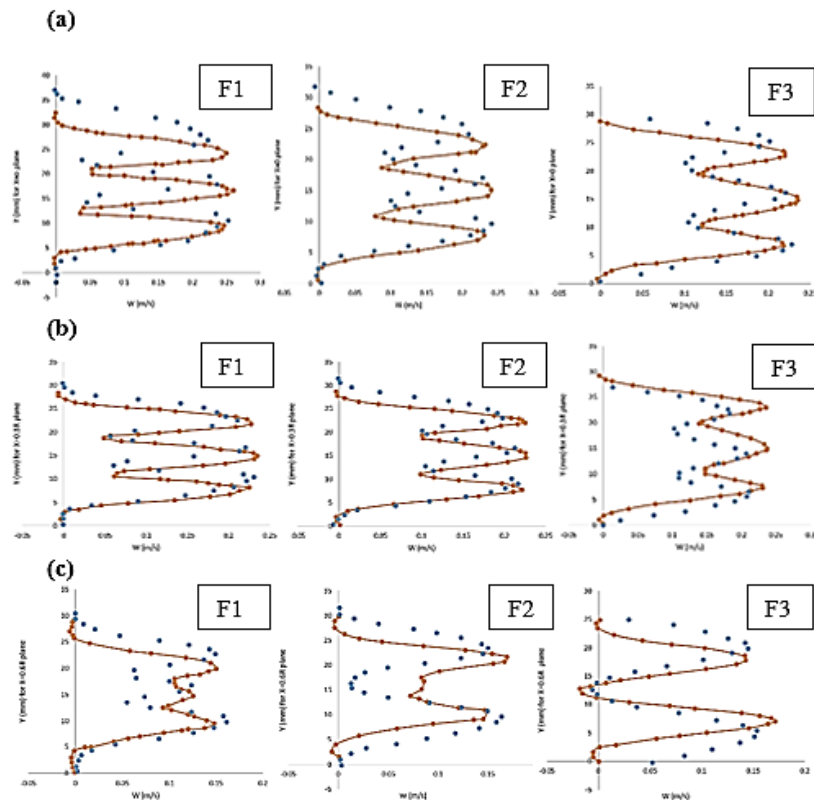
(a)

(b)

(c)

Fig. 6. Velocity profile comparison between previous study and CFD method for (a) X=0 (b) X=0.3R mm (c) X=0.6R mm plane position (previous study – PIV [4, 5], Present CFD method).

The graph showed that the numerical simulation was essentially accurate in all features observed in the experiment. The complex transverse distribution of the momentum within the cross section and the rate at which the three jets diffuse and merge in stream-wise direction.

4. Results and Discussion

The numerical simulation for laminar flow regime at Re = 750 was conducted with the SJM valve at a fully open position. This study aimed to investigate and understand the effect of using VG as a method in reducing blood clots. Validating the numerical method is essentially important to achieve accurate flow physics. The laminar flow regimes were repeated with different triangular VG arrangements to obtain the pressure losses with and without VG. Figure 7 shows the velocity contour and vector for the different arrangements of triangular VGs. The instantaneous stream-wise velocity at x=0 plane (symmetry plane perpendicular to the leaflets). The highest max velocity among VG arrangement was found in an equally triangular VG at 0.291 m/s, followed by straight triangular VG at 0.286 m/s and without VG at 0.282 m/s. A velocity with a smaller value could lead to blood clotting [18]. For straight triangular VG, the blood flow seemed to have a uniform velocity compared to the equally triangular VG.
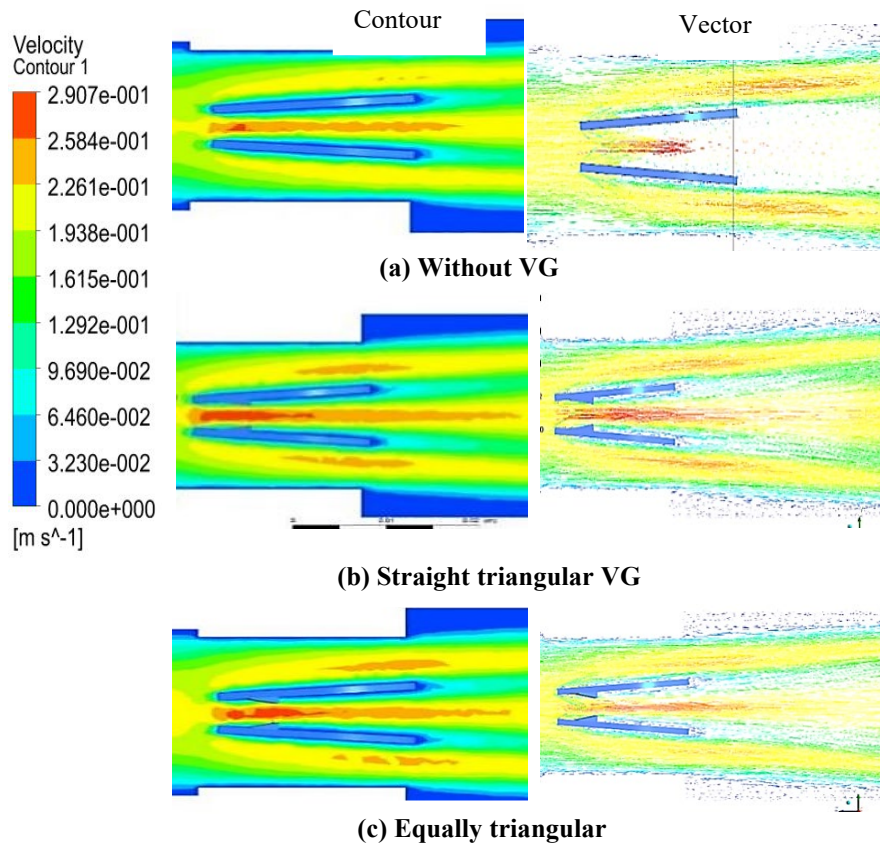
**Fig. 7. Velocity contour and vector for
VG leaflet at different arrangements of VGs.**

Moreover, the velocity vector is responsible for the combination of vortex shedding where the wake is produced at the trailing edge of VGs [19]. The direction of the blood flow within sinuses and from leaflet could determine from velocity vector representation [20]. The vortex normally encountered in the bluff body and sharp edge due to inertia. The detail analysis through computational study can improve the design of MHV which is the vortices can be reduced then the blood clotting can be prevented [21]. Figure 8 shows the velocity profile comparison of triangular VGs configuration. The blood flow through BMHV without VG seemed to have non-uniform velocity than having VGs.

The effect of using triangular VG with different arrangements can be measured by calculating the non-dimensional ΔP coefficient equation to find pressure loss through VGs. The identification of the location of the inlet and outlet pressures are shown in Fig. 9. The pressure drop value was identified by using Fig. 9, as a guide for obtaining the value of pressure loss. The pressure drops were calculated to determine the value of decreasing blood clots. The pressure losses were calculated with and without triangular VG. The values of inlet and outlet pressures were collected from the numerical simulation under steady state conditions.
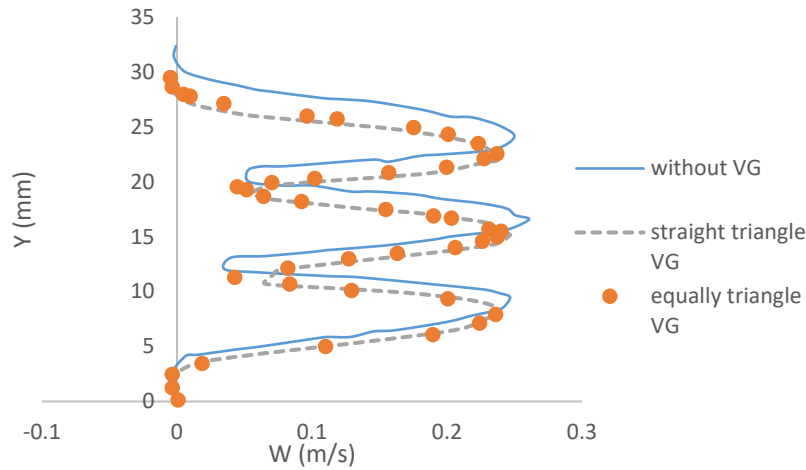
**Fig. 8. Velocity profile comparison with VG (—— without VG
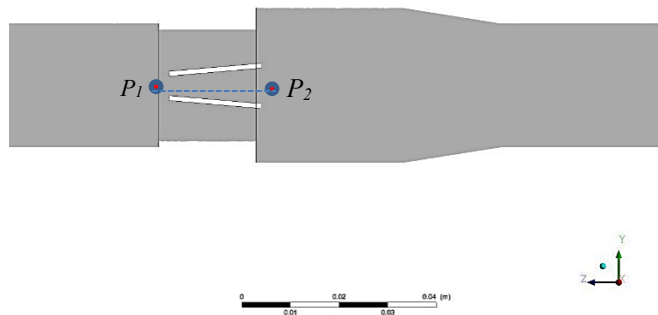---- straight triangular VG ● equally triangular VG)**

Fig. 9. Pressure drop, $\Delta P = P_1 - P_2$

Table 1 demonstrates that less pressure drop across the heart valves indicates the small obstruction area. Therefore, a good efficiency of the heart valve can be obtained. The blood flow through vessel or across the heart valve have a force propelling the blood which this force is the difference in blood pressure. The result of pressure drop tended to increase from 0% to 5.3% with straight triangular VG and 2.7% for equally triangular VG. The development of blood clotting increases with increasing pressure drop. A similar phenomenon occurs with increasing velocity. The rotating motion of blood particles increases at the same spot, and the probability of blood accumulation reduce thrombus development.

Table 1. Data for the pressure drop.

	Without VG	Straight triangular VG	Equally triangular VG
P_1	24.5699 Pa	24.041 Pa	24.526 Pa
P_2	10.059 Pa	10.303 Pa	10.402 Pa
ΔP	1.165	1.103	1.134
Percentage, %	0	5.3%	2.7%

5. Conclusions

In this study, the blood flow through BMHV is analysed at different arrangement of triangular VGs. Results suggested that using VGs could affect the performance of BMHV flow. For instance, as BMHV equipped with triangular VGs, the maximum velocity magnitude increases from 0.25 m/s to 0.28 m/s in the middle for straight triangular VGs configuration. Higher velocities and flow separation at the leaflet surface were accompanied by growing eddies and vorticity downstream of the valve. The pressure drop was found to increase from 0% to 5.3% for straight triangular VGs. Even though pulsatile flow, turbulent flow and motion of the leaflets were not considered in this paper, the study comprises an important step toward the development of a numerical simulation structure for MHV flows. This study also yielded a validated and reliable flow solver, which can help further investigation to tackle the next level complexity. Therefore, further studies are needed in improving the method or geometry to obtain satisfactory results.

Acknowledgement

Nomenclatures	
D	Diameter of the valve, mm
Re	Reynolds number
r	Radius of valve, mm
$\vec{V}$	Velocity vector, m/s
V_{avg}	Average velocity, m/s
V_{max}	Maximum velocity, m/s
ΔP	Pressure drop, Pa
Abbreviations	
BMHV	Bileaflet Mechanical Heart Valve
CFD	Computational Fluid Dynamics
NS	Navier-Stokes
RMS	Root mean square
SIMPLE	Semi-Implicit Method Pressure Linked Equations
VG	Vortex Generator

References

1. Dasi, L.P.; Simon, H.A.; Sucosky, P.; and Yoganathan, A.P. (2009). Fluid mechanics of artificial heart valves. *Clinical Experimental Pharmacology and Physiology*, 36(2), 225-237.
2. Yun, B.M.; Wu, J.; Simon, H.A.; Arjunon, S.; Sotiropoulos, F.; Aidun, C.K.; and Yoganathan, A.P (2012). A numerical investigation of blood damage in the hinge area of aortic bileaflet mechanical heart valves during the leakage phase. *Annals of Biomedical. Engineering*, 40(7), 1468-1485.

3. Zakaria, M.S.; Ismail, F.; Tamagawa, M.; Aziz, A.F.A.; Wiriadidjaja, S.; Basri, A.A.; and Ahmad, K.A. (2017). Review of numerical methods for simulation of mechanical heart valves and the potential for blood clotting. *Medical Biological Engineering Computing*, 55, 1519-1548.

4. Yun, B.M.; Dasi, L.P.; Aidun, C.K.; and Yoganathan, A.P. (2014). Computational modelling of flow through prosthetic heart valves using the entropic lattice-Boltzmann method. *Journal of Fluid Mechanics*, 743, 170-201.

5. Ge, L.; Leo, H.L.; Sotiropoulos, F.; and Yoganathan, A.P. (2005). Flow in a mechanical bileaflet heart valve at laminar and near-peak systole flow rates: CFD simulations and experiments. *Journal Biomechanical Engineering*, 127(5), 782-797.

6. Bark Jr, D.L.; Vahabi, H.; Bui, H.; Movafaghi, S.; Moore, B,; Kota, A.K.; Popat, K.; and Dasi, L.P. (2017) Hemodynamic performance and thrombogenic properties of a superhydrophobic bileaflet mechanical heart valve. *Annals Biomedical Engineering*, 45(2), 452-463.

7. Dasi, L.P.; Murphy, D.W.; Glezer, A.; and Yoganathan, A.P. (2008). Passive flow control of bileaflet mechanical heart valve leakage flow. *Journal Biomechanics*, 41(6), 1166-1173.

8. Hatoum, H.; and Dasi, L.P. (2019). Reduction of pressure gradient and turbulence using vortex generators in prosthetic heart valves. *Annals of Biomedical Engineering*, 47(1), 85-96.

9. Sudhamshu, A.R.; Pandey, M.C.; Sunil, N.; Satish, N.S.; Mugundhan, V.; and Velamati, R.K. (2016). Numerical study of effect of pitch angle on performance characteristics of a HAWT. *Engineering Science Technology an International Journal*, 19(1), 632-641.

10. Dutta, P.; Saha, S.K.; Nandi, N.; and Pal, N. (2016). Numerical study on flow separation in 90° pipe bend under high Reynolds number by k-ε modelling. *Engineering Science Technology an International Journal*, 19(2), 904-910.

11. Oh, H.S.; Kang, S.H.; Nam, S.H.; Kim, E.J.; and Hwang, T.M. (2019). CFD modelling of cyclonic-DAF (dissolved air flotation) reactor for algae removal. *Engineering Science Technology an International Journal*, 22(2), 477-481.

12. Wendt, J. (2009). *Computational fluid dynamics: An introduction*. New York: Springer-Verlag.

13. Chirica, I.; Angheluta, C.M.; Perijoc, S.D.; Hobjila, A.I.; and Fratita, M. (2019). Mesh independence of a transient multiphase fluid-solid interaction. *Journal of Physics: Conference Series*, 1297, 012026.

14. Zakaria, M.S.; Ismail, F.; Tamagawa, M.; Aziz, A.F.A.; Wiriadidjaja, S.; Basri, A.A.; and Ahmad, K.A. (2018). Computational fluid dynamics study of blood flow in aorta using OpenFOAM. *Journal Advance Research Fluid Mechanical Thermal, Science*, 43(1), 81-89.

15. Zou, Q.; and He, X. (1997). On pressure and velocity boundary conditions for the lattice Boltzmann BGK model. *Physics of Fluids*, 9(6), 1591-1598.

16. Sotiropoulos, F.; Le, T.B.; and Gilmanov, A. (2015). Fluid mechanics of heart valves and their replacements. *Annual Review of Fluid Mechanics*, 48(1), 259-283.

17. Su, B.; Kabinejadian, F.; Phang, H.Q.; Kumar, G.P.; Sangho, C.; Kim, S.; Tan, R.S.; Hon, J.K.F.; Allen, J.C.; Leo, H.L.; and Zhong, L. (2015). Numerical

modeling of intraventricular flow during diastole after implantation of BMHV. *PLOS ONE*, 10(5): e0126315.

18. Fogelson, A.L.; and Neeves, K.B. (2015). Fluid mechanics of blood clot formation. *Annual Review of Fluid Mechanics*, 47, 377-403.

19. Salleh, N.M.; Zakaria, M.S.; and Abd Latif, M.J. (2019). The vortex shedding for an inclined flat plate of thrombosis using CFD simulation. *Proceedings of Mechanical Engineering Research Day*. Melaka, Malaysia, 152-154.

20. Amindari, A.; Saltik, L.; Kirkkopru, K.; Yacoub, M.; and Yalcin, H.C. (2017). Assessment of calcified aortic valve leaflet deformations and blood flow dynamics using fluid-structure interaction modeling. *Journal of Informatics in Medicine Unlocked*, 9, 191-199.

21. Zhen, T.K.; Zubair, M.; and Ahmad, K.A. (2011). Experimental and numerical investigation of the effects of passive vortex generators on Aludra UAV performance. *Chinese Journal of Aeronautics*, 24(5), 577-583.